11th International Workshop on Computational Electronics
TU Wien, 25-27 May 2006

3D Monte-Carlo Device Simulations Using an Effective Quantum Potential Including Electron-Electron Interactions

Clemens Heitzinger, Christian Ringhofer, Shaikh Ahmed*, and Dragica Vasileska*
Department of Mathematics, Arizona State University, Tempe, AZ 85287, USA
*Department of Electrical Engineering, Arizona State University, Tempe, AZ 85287, USA
E-mail: Clemens.Heitzinger@asu.edu

The Effective Quantum Potential

As device sizes decrease, the standard mean-field theory for the treatment of electron-electron forces becomes less applicable. Motivated by this fact, effective quantum potentials have been established as a proven way to include quantum-mechanical effects into Monte-Carlo (MC) device simulations. The pseudo-differential operator for the effective quantum potential we build on here is based on a perturbation theory around thermal equilibrium [1], [2] and was first derived in [3]. The approach was generalized in [4] to the general N-body problem, i.e., particle-particle interactions. In this work we present 3D MC device simulation results obtained from this formulation.

Simulation Results and Discussion

The effective quantum potential is shown in Fig. 1 and Fig. 2. The SOI device used here (Fig. 3) has the following specifications: gate length is 10nm, the source/drain length is 15nm each, the thickness of the silicon on insulator (SOI) layer is 7nm, with p-region width of 10nm makes it a fully-depleted device under normal operating conditions, the gate oxide thickness is 0.8nm, the box oxide thickness is 140nm, the channel doping is uniform at $1.45 \cdot 10^{10}\mathrm{cm}^{-3}$ (intrinsic/undoped), the doping of the source/drain regions equals $5 \cdot 10^{19}\mathrm{cm}^{-3}$, and the gate is assumed to be a metal gate with a work-function adjusted to 4.188. The device is designed in order to achieve the ITRS performance specifications for the year 2016.

The distribution function (Fig. 4) shows that inclusion of quantum potential leads to an increase of the high energy tail of the electron distributions at the transition from channel to drain.

The simulated output characteristics are shown in Fig. 5 with an applied gate bias of 0.4V. Noticeable is the reduced short-channel effects even with an extremely low channel doping density. Inclusion of quantum potential significantly reduces the drive current and transconductance and increases the device threshold voltage as observed from the slope of the linear region. One can also see that the impact of quantization effects reduces as the drain voltage increases (increase in energy) because of the growing bulk nature of the channel electrons.

Conclusion

We showed the applicability of a novel effective quantum potential not using any fitting parameters for the N-body problem to 3D MC device simulations. The inclusion of particle-particle interactions, as opposed to the classical Coulomb potential, shows a notable difference in the current-voltage characteristics.

Acknowledgment

The authors acknowledge support by the Austrian Science Fund (Fonds zur Förderung der wissenschaftlichen Forschung, FWF) and through National Science Foundation grant DECS-0218008.

References

[1] I. Gasser and A. Jüngel. *Z. Angew. Math. Phys.*, 48:45–59, 1997.
[2] C.L. Gardner and C. Ringhofer. *Physical Review*, E53:157–167, 1996.
[3] C. Ringhofer, C. Gardner, and D. Vasileska. *Inter. J. on High Speed Electronics and Systems*, 13(3):771–801, 2003.
[4] C. Heitzinger and C. Ringhofer. *Journal of Computational Electronics*, 2005. *(Submitted for publication).*

ISBN 3-901578-16-1

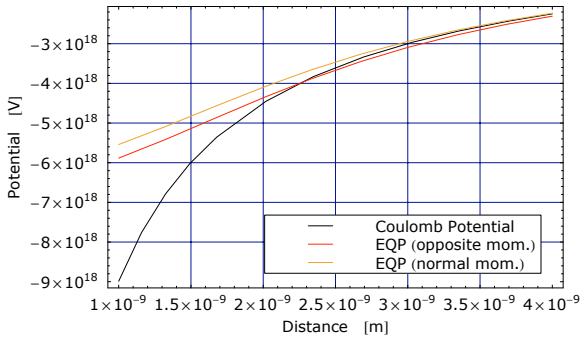

Fig. 1. The effective quantum potential (EQP) compared the Coulomb potential. For the EQP the momentum vectors are $(p,0,0)$ and $(-p,0,0)$ for the opposite momentum curve and $(p,0,0)$ and $(0,p,0)$ for the normal momentum case where $p := 5.40275 \cdot 10^{-26}$.

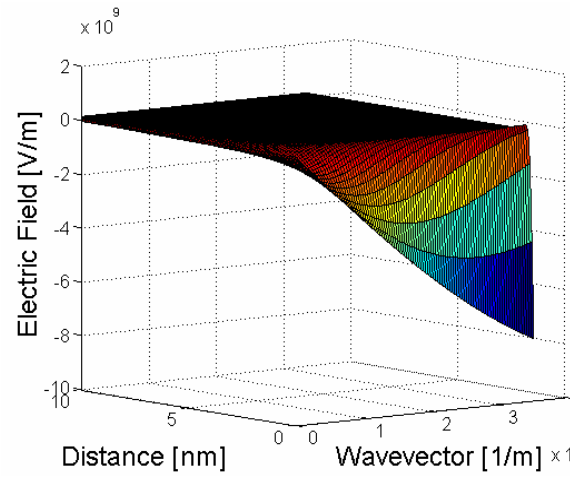

Fig. 2. The effective quantum potential due to the barrier.

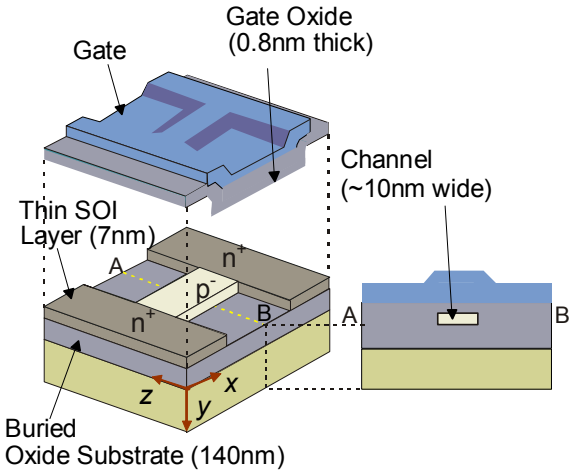

Fig. 3. The structure of the simulated 3D device.

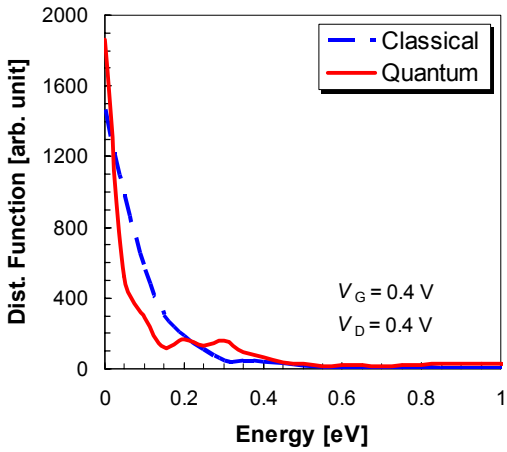

Fig. 4. Distribution function.

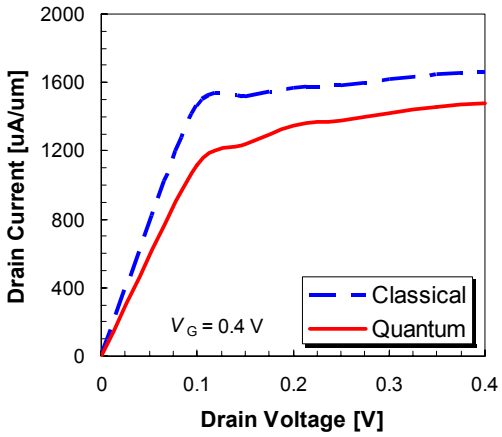

Fig. 5. Current-voltage characteristics for a gate bias of 0.4V.

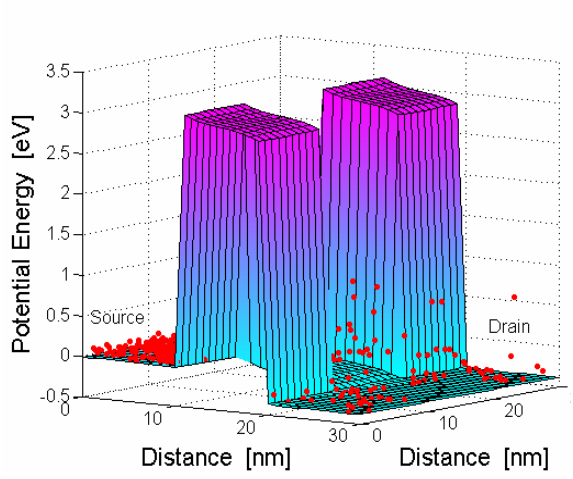

Fig. 6. The electron distribution in the device during the simulation.